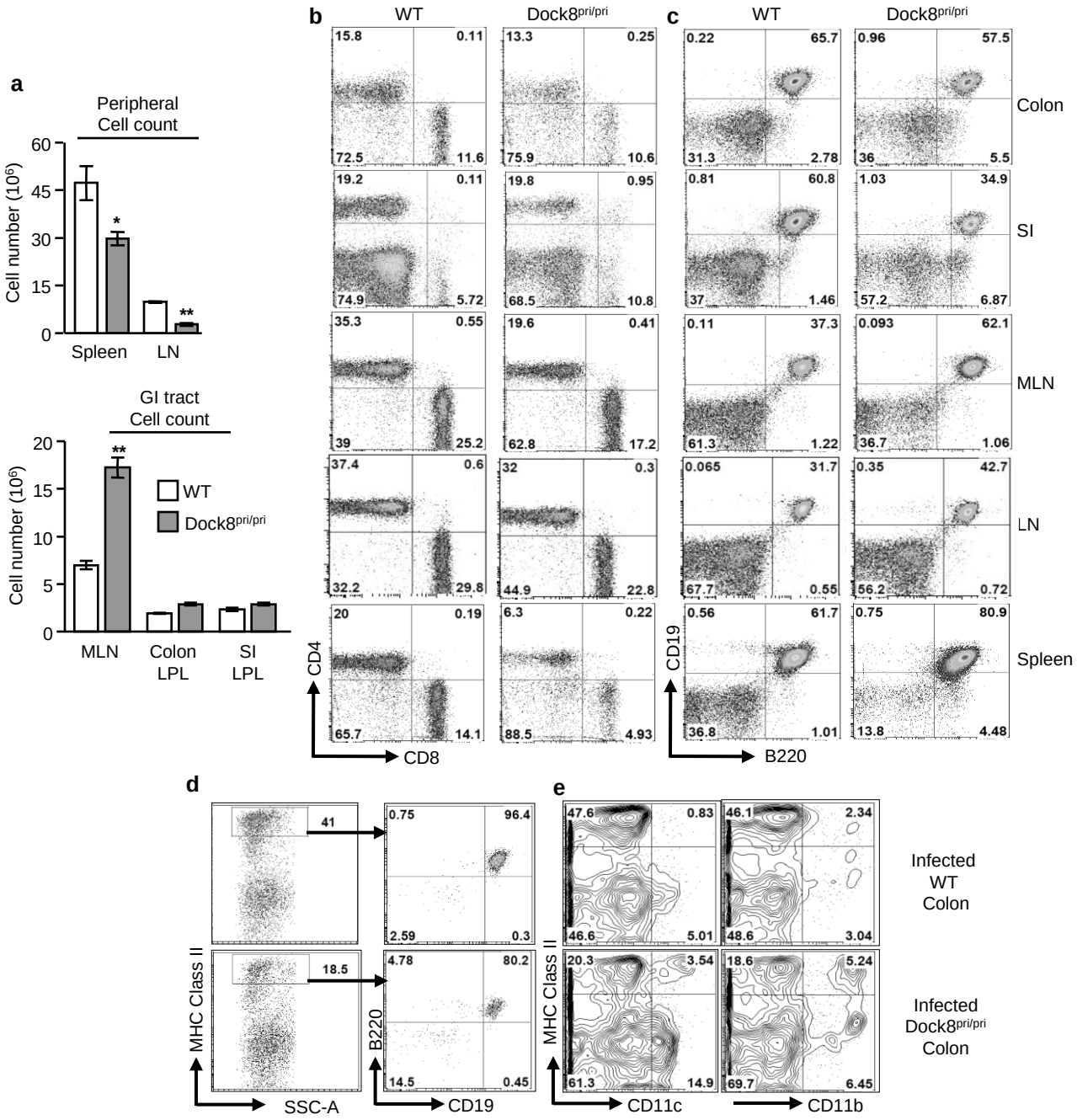

Supplementary Figure 1 DOCK8 is required for the recruitment of MHC class II^{high} B cells to the colon after infection with enteric pathogen, related to figure 1. Total lymphocytes were isolated from spleen, LN, MLN, colon, and SI of WT and DOCK8$^{pri/pri}$ mice and analyzed by flow cytometry. **(a)** Graphs showing the absolute number of lymphocytes in different organs. **(b and c)** The representative dot plots showing the CD4^{+}, CD8^{+}, CD19^{+} and B220^{+} populations in different organs. **(d)** Colonic LPLs were isolated from *C. rodentium* infected mice at day 8 *p.i*. The left panel shows representative dot plots of MHC Class II^{high} and the right panel shows the percentage of CD19^{+} and B220^{+} cells among total MHC Class II^{high} cells. **(e)** Representative dot plots showing that DOCK8 deficient mice do not have a defect in the recruitment of CD11b^{+} or CD11c^{+} cells to the colon of infected mice. Three independent experiments were performed with three mice per group. The data shown are the mean ± SD. P-values were obtained by student's t-test. *ns* = p> 0.05, *p< 0.05, **p< 0.01.

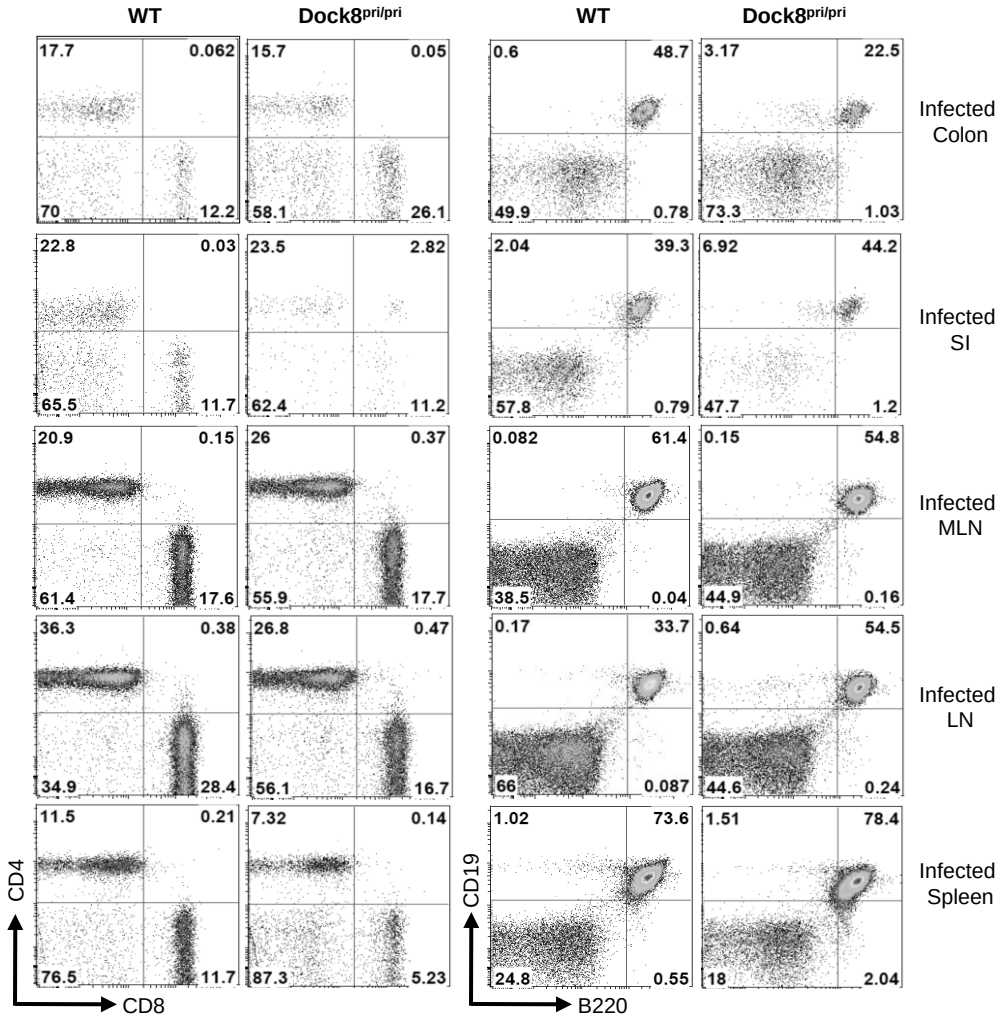

Supplementary Figure 2 DOCK8 is required for the recruitment of B cells to the colon after infection with enteric pathogen, related to figure 1. Total lymphocytes were isolated from spleen, LN, MLN, colon and SI of WT and Dock8$^{pri/pri}$ mice at day 8 *p.i.* and analyzed by flow cytometry. **(Left)** The representative dot plots showing the CD4^{+} and CD8^{+} cells in different organs. **(Right)** The representative dot plots showing the CD19^{+} and B220^{+} populations in different organs. Two independent experiments were performed with three mice per group.

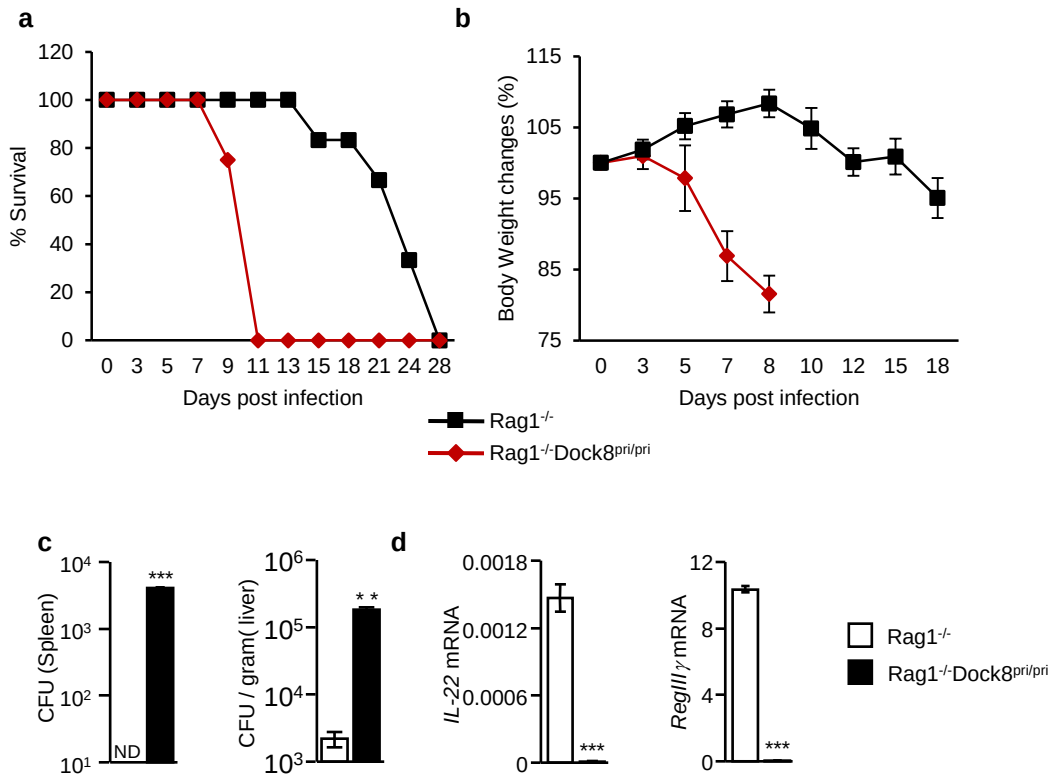

Supplementary Figure 3 DOCK8 is critical for innate immune cell mediated protection against enteric pathogen, related to figure 1. Rag1$^{-/-}$ or Rag1$^{-/-}$Dock8$^{pri/pri}$ mice were infected with *C. rodentium.* **(a)** Percent survival and **(b)** average body weight change after infection. Rag1$^{-/-}$ or Rag1$^{-/-}$Dock8$^{pri/pri}$ mice were infected with *C. rodentium* and sacrificed on day 8 post infection. **(c)** CFU in the spleens and livers of infected mice. **(d)** Colonic *IL-22 and RegIIIγ* expressions in response to infection. Three independent experiments were performed with a minimum of four mice per group. The data shown are the mean ± SD. P-values were obtained by student's t-test. **p< 0.01, **p< 0.001.*ns* = not significant.

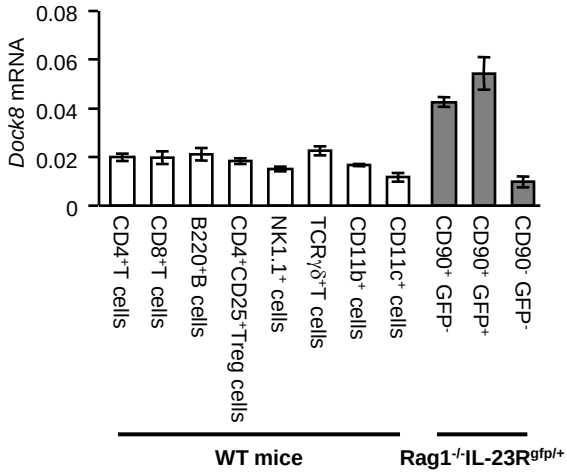

Supplementary Figure 4 *Dock8* message is highly expressed in ILCs, related to figure 3. Indicated cell types were sorted from spleens of WT and GI tract LPLs of Rag1$^{-/-}$IL-23R$^{gfp/+}$ mice. Total RNA was extracted from purified cells with Trizol and reverse transcribed with the iScript cDNA synthesis kit. The real time PCR was conducted using step one plus real time PCR system with TaqMan Gene Expression Assay Mm00613802 (Applied Biosystems). Two independent experiments were performed with a pooled samples from three mice.

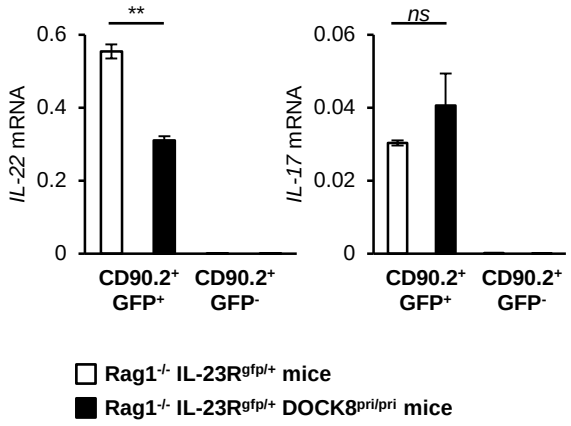

Supplementary Figure 5 Remaining DOCK8 deficient ILC3 have reduced expression of *IL-22* but normal expression of *IL-17A*, related to figure 3. CD90.2$^+$IL-23R$^-$ and CD90.2$^+$IL-23R$^+$ (ILC3) cells were purified from the SI LPLs of Rag1$^{-/-}$IL-23R$^{gfp/+}$ and Rag1$^{-/-}$IL-23R$^{gfp/+}$DOCK8$^{pri/pri}$ mice. Total RNA was extracted from purified cells with RNeasy mini kit (Qiagen) and reverse transcribed with the iScript cDNA synthesis kit (BioRad). The real time PCR was conducted using primers and probe as depicted in Table S1. Gene expression was normalized as n-fold difference to the gene *RPL-19*. Two independent experiments were performed with a pooled samples from four mice per group. The data shown are the mean ± SD. P-values were obtained by student's t-test. **p< 0.01.

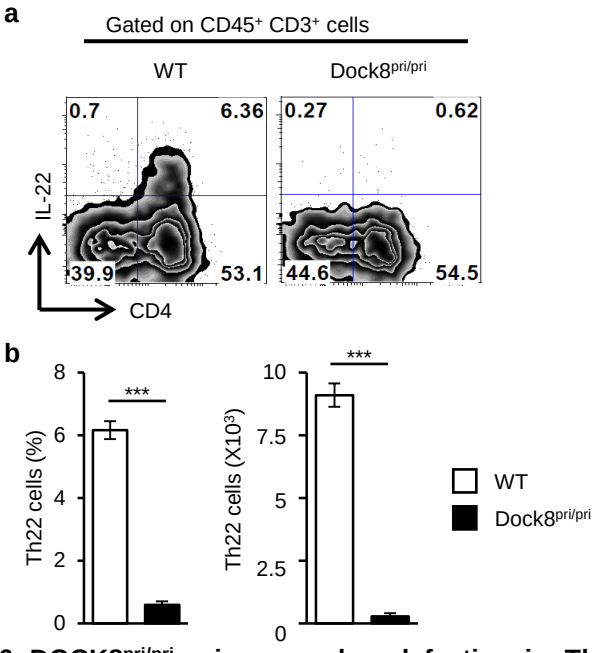

Supplementary Figure 6 DOCK8$^{pri/pri}$ mice are also defective in Th22 response against *C. rodentium*, related to figure *3*. WT and DOCK8$^{pri/pri}$ mice were infected with 2 x 10^9 CFU of *C. rodentium* **(a)** CD45$^+$CD3$^+$CD4$^+$ T cells were analyzed for IL-22 production in colonic LPLs at day eight post *infection* by flow cytometry. **(b)** Percentage and absolute numbers of IL-22$^+$ T cells. Two independent experiments were performed with three mice per group. The data shown are the mean ± SD. P-values were obtained by student's t-test. ***p< 0.001.

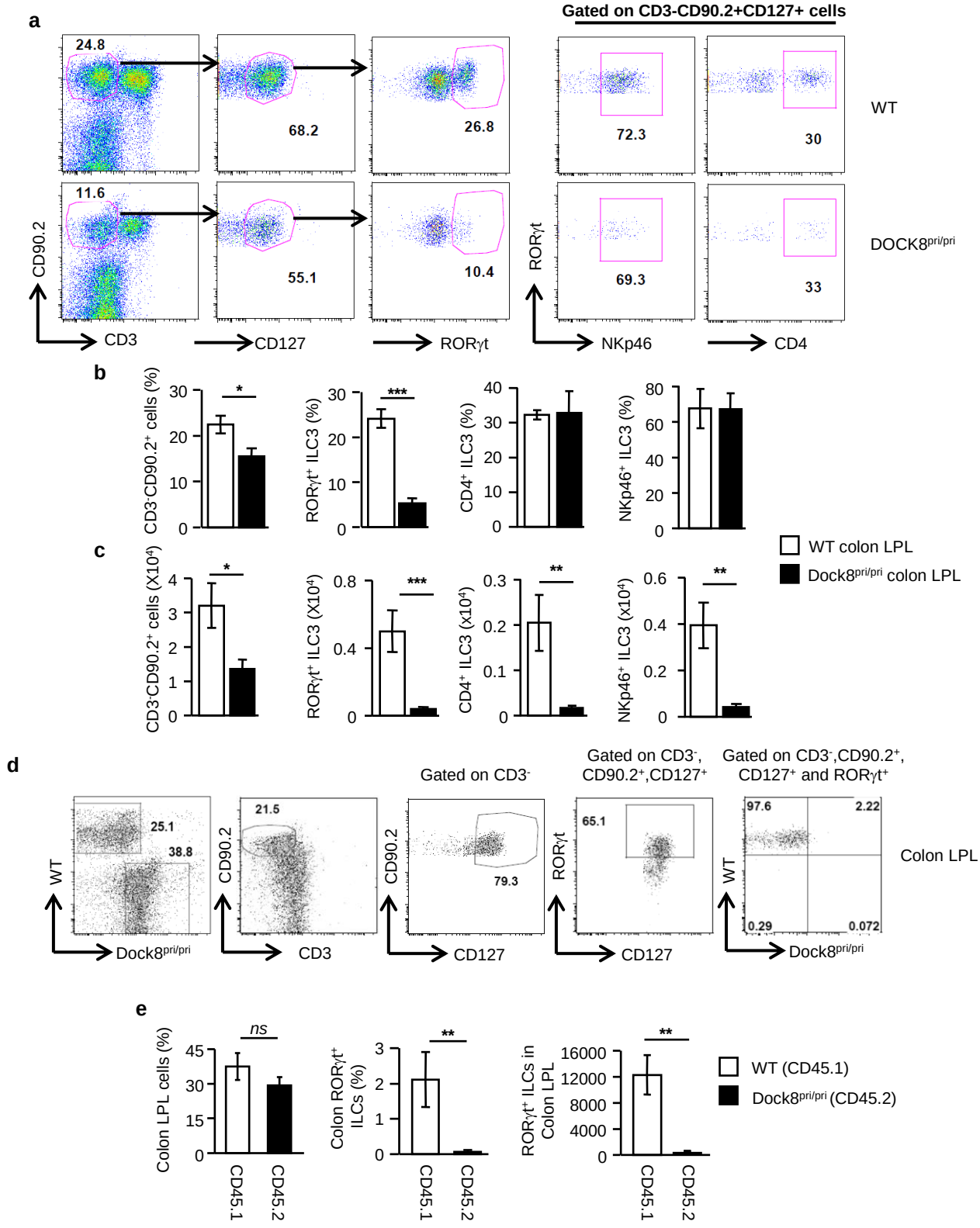
a
Gated on CD3-CD90.2+CD127+ cells
24.8
68.2
26.8
11.6
55.1
10.4
72.3
30
69.3
33
WT
DOCK8pri/pri
CD90.2
CD3
CD127
RORγt
NKp46
CD4
b
CD3-CD90.2+ cells (%)
RORγt+ ILC3 (%)
CD4+ ILC3 (%)
NKp46+ ILC3 (%)
c
CD3-CD90.2+ cells (X10⁴)
RORγt+ ILC3 (X10⁴)
CD4+ ILC3 (x10⁴)
NKp46+ ILC3 (x10⁴)
WT colon LPL
Dock8pri/pri colon LPL
d
Gated on CD3-
Gated on CD3-, CD90.2+,CD127+
Gated on CD3-,CD90.2+, CD127+ and RORγt+
25.1
38.8
21.5
79.3
65.1
97.6
2.22
0.29
0.072
WT
Dock8pri/pri
CD90.2
CD3
CD127
RORγt
Colon LPL
e
ns
Colon LPL cells (%)
Colon RORγt+ ILCs (%)
RORγt+ ILCs in Colon LPL
CD45.1
CD45.2
WT (CD45.1)
Dock8pri/pri (CD45.2)

Supplementary Figure 7 Profound reduction of RORγt$^+$ ILCs in the absence of DOCK8, related to figure 4. **(a)** RORγt$^+$ ILCs were analyzed in colonic LPLs by flow cytometry after gating on CD3$^-$CD90.2$^+$CD127$^+$ cells. **(b and c)** Percentage and absolute numbers of CD3$^-$CD90.2$^+$, CD3$^-$CD90.2$^+$CD127$^+$RORgt$^+$, CD3$^-$CD90.2$^+$CD127$^+$RORgt$^+$CD4$^+$ and CD3$^-$CD90.2$^+$CD127$^+$RORgt$^+$ NKp46$^+$ cells of WT and DOCK8$^{pri/pri}$ mice. **(d and e)** Cell intrinsic functions of DOCK8 regulate RORγt$^+$ ILCs. Mixed bone marrow chimeras generated by reconstituting 50% CD45.1 WT and 50% CD45.2 DOCK8$^{pri/pri}$ mice and transferred into lethally irradiated Rag2$^{-/-}$ IL-2Rgc$^{-/-}$ mice. **(d)** RORγt$^+$ ILCs (CD3$^-$CD90.2$^+$CD127$^+$) were analyzed in the colonic LPLs four weeks post transfer. **(e)** The percentage and absolute number of RORγt$^+$ ILCs. Three independent experiments were performed with a minimum of three mice per group. The data shown are the mean ± SD. P-values were obtained by student's t-test. **p< 0.01, ***p< 0.001. ns = not significant.

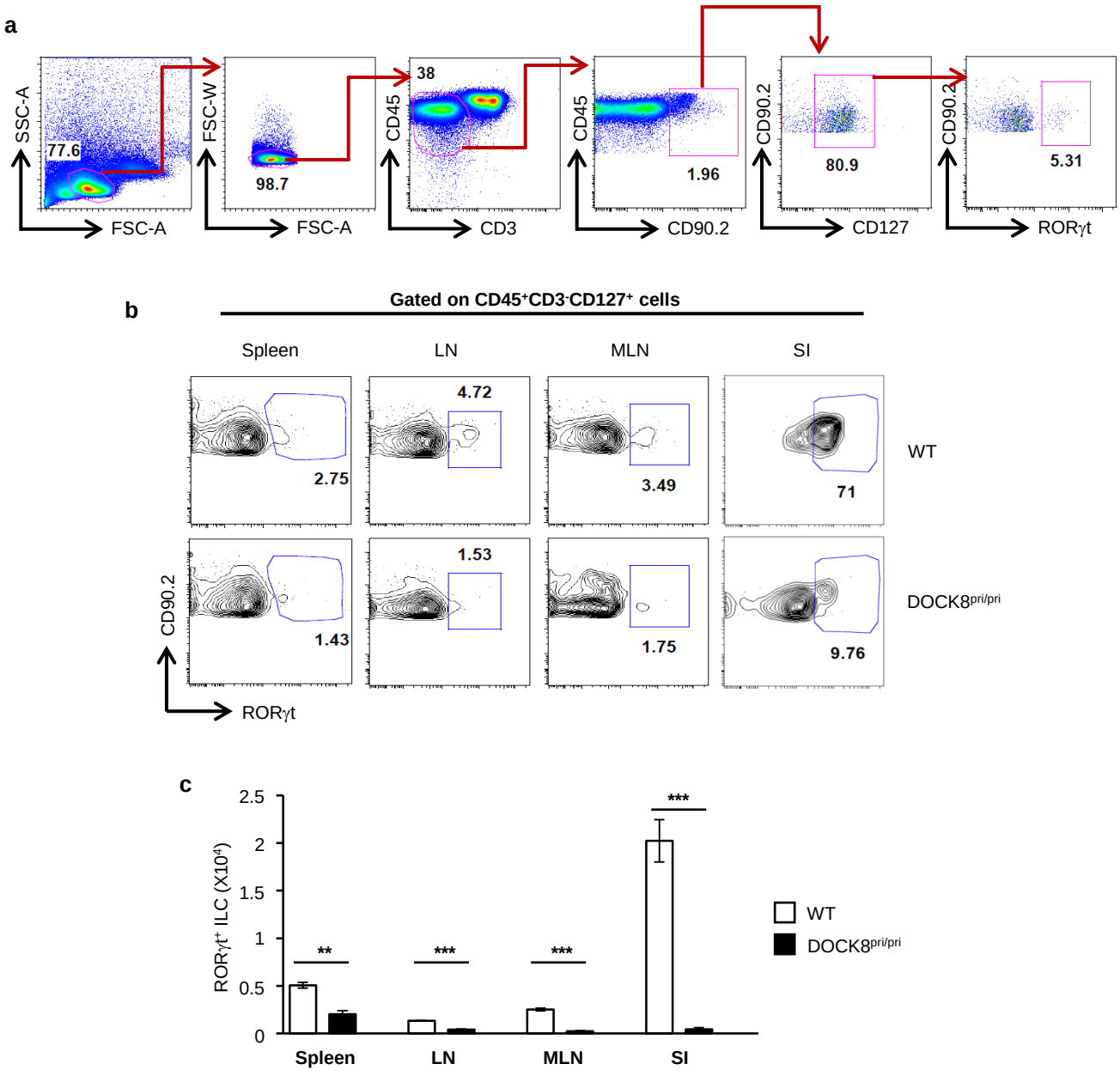

Supplementary Figure 8 Reduction of RORγt⁺ ILCs in the absence of DOCK8 is not only limited to gut, related to figure 4. (a) Gating strategy for RORγt⁺ ILC3 in the spleen, lymph nodes (LN), mesenteric lymph nodes (MLN) and small intestine (SI). **(b)** RORγt⁺ ILCs were analyzed in spleen, LN, MLN and SI by flow cytometry after gating on CD45⁺CD3⁻CD90.2⁺CD127⁺ cells. **(c)** Absolute numbers of CD45⁺CD3⁻CD90.2⁺CD127⁺RORγt⁺ cells of WT and DOCK8$^{pri/pri}$ mice. Two independent experiments were performed with three mice per group. The data shown are the mean ± SD. P-values were obtained by student's t-test. *p< 0.05, **p< 0.01, ***p< 0.001.

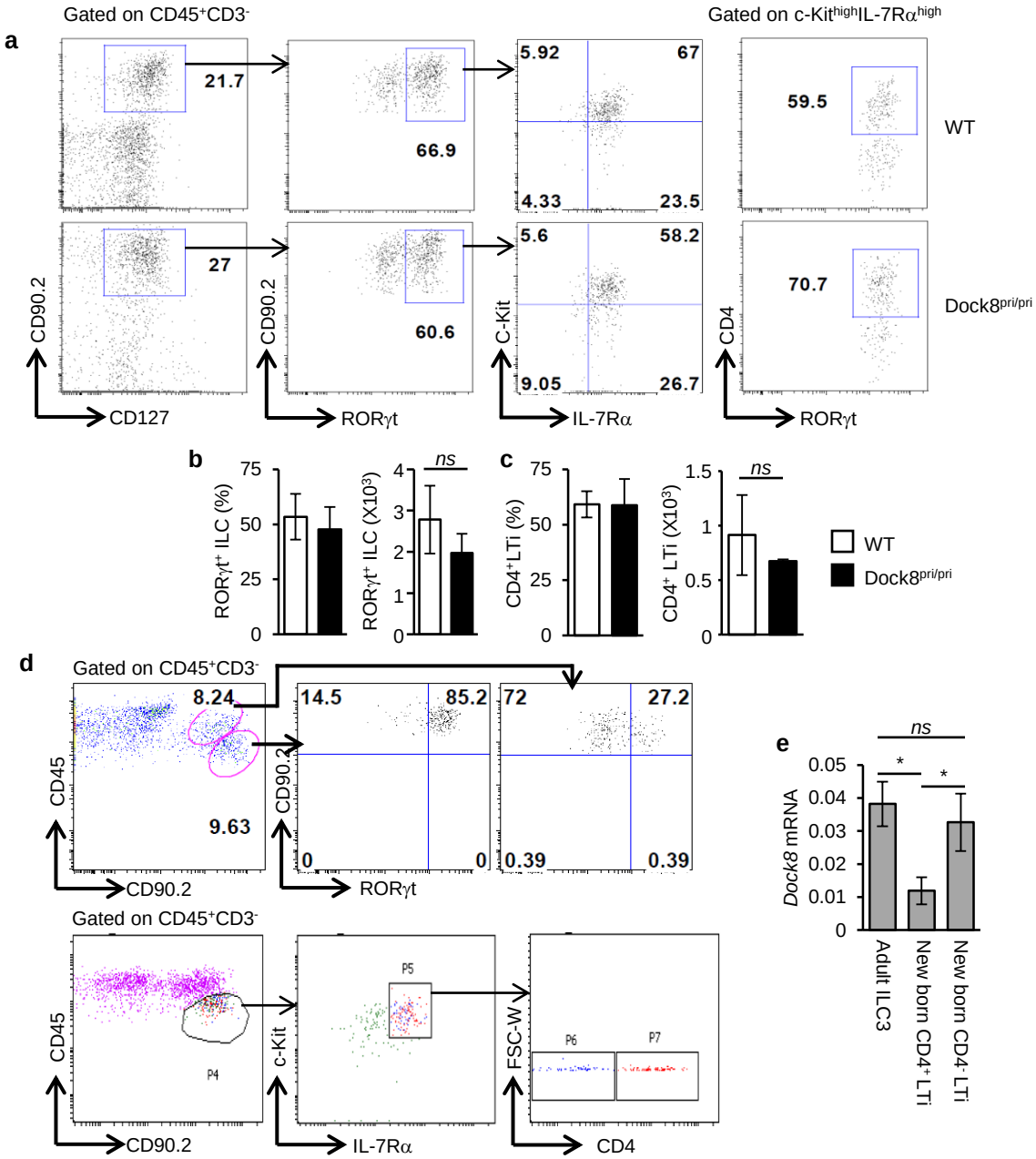

Supplementary Figure 9 Perinatal LTi cells are normal in DOCK8$^{pri/pri}$ mice, related to figure 4. (a) perinatal LTi cells were analyzed in the GI tract of WT and DOCK8$^{pri/pri}$ new born mice by flow cytometry after gating on CD45$^+$CD3$^-$CD90.2$^+$CD127$^+$ RORγt$^+$ c-Kit^{high} IL-7Rα^{high} CD4$^+$ or CD4$^-$ cells. **(b)** Percentage and absolute numbers of perinatal RORγt$^+$ ILCs and **(c)** Percentage and absolute numbers of perinatal CD4$^+$ LTi cells. Two independent experiments were performed with 6 mice per group. **(d upper panel)** CD3$^-$CD45^{low}CD90^{high} cells are mostly RORγt$^+$. **(d lower panel)** Gating strategy for perinatal LTi cells sorting from WT mice. **(e)** Indicated cell types were sorted from GI tract LPLs of WT mice. Total RNA was extracted from purified cells with Trizol and reverse transcribed with the iScript cDNA synthesis kit. The real time PCR was conducted using step one plus real time PCR system with TaqMan Gene Expression Assay Mm00613802 (Applied Biosystems). Two independent experiments were performed with pooled samples from five new born mice. The data shown are the mean ± SD. P-values were obtained by student's t-test. *p< 0.05. *ns* = not significant.

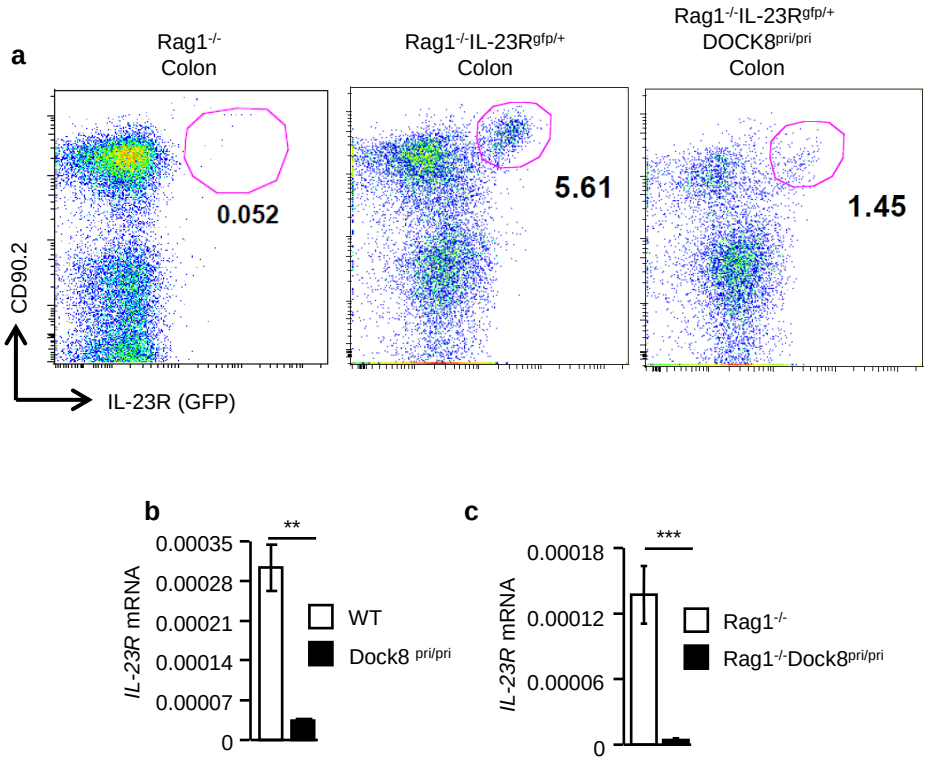

Supplementary Figure 10 Profound reduction of IL-23R^{+} ILCs in the absence of DOCK8, related to figure 4. (a) IL-23R^{+} ILCs were analyzed in the colonic LPLs isolated from Rag1$^{-/-}$, Rag1$^{-/-}$ IL-23R$^{gfp/+}$ and Rag1$^{-/-}$ IL-23R$^{gfp/+}$DOCK8$^{pri/pri}$ mice at day 8 post infection. **(b)** Colonic *IL-23R* expression in colons of WT and DOCK8$^{pri/pri}$ mice at day 8 p.i. **(c)** Colonic *IL-23R* expression in colons of Rag1$^{-/-}$ and Rag1$^{-/-}$ DOCK8$^{pri/pri}$ mice at day 8 p.i. Two independent experiments were performed with three mice per group. The data shown are the mean ± SD. P-values were obtained by student's t-test. **p< 0.01, ***p< 0.001. *ns* = not significant.

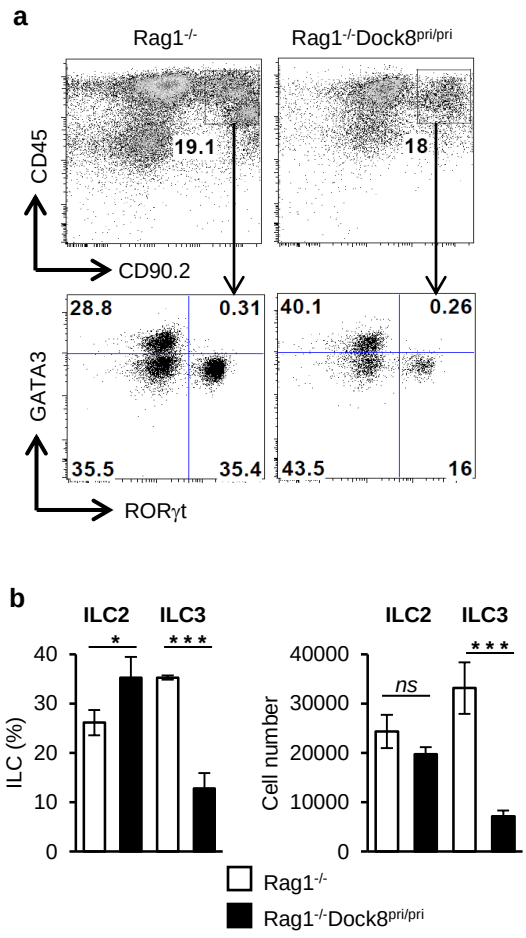

Supplementary Figure 11 DOCK8 deficiency does not affect ILC2 in the gut, related to figure 4. (a) RORγt$^+$ ILCs (ILC3) and GATA3$^+$ ILCs (ILC2) were analyzed in the small intestine of Rag1$^{-/-}$ and Rag1$^{-/-}$DOCK8$^{pri/pri}$ mice by flow cytometry after gating on CD45$^+$CD90.2$^+$ cells. **(b)** Absolute numbers of CD45$^+$CD90.2$^+$GATA3$^+$ (ILC2) and CD45$^+$CD90.2$^+$RORγt$^+$ (ILC3) cells of Rag1$^{-/-}$ and Rag1$^{-/-}$DOCK8$^{pri/pri}$ mice . Three independent experiments were performed with three mice per group. The data shown are the mean ± SD. P-values were obtained by student's t-test. *p< 0.05, ***p< 0.001. *ns* = not significant.

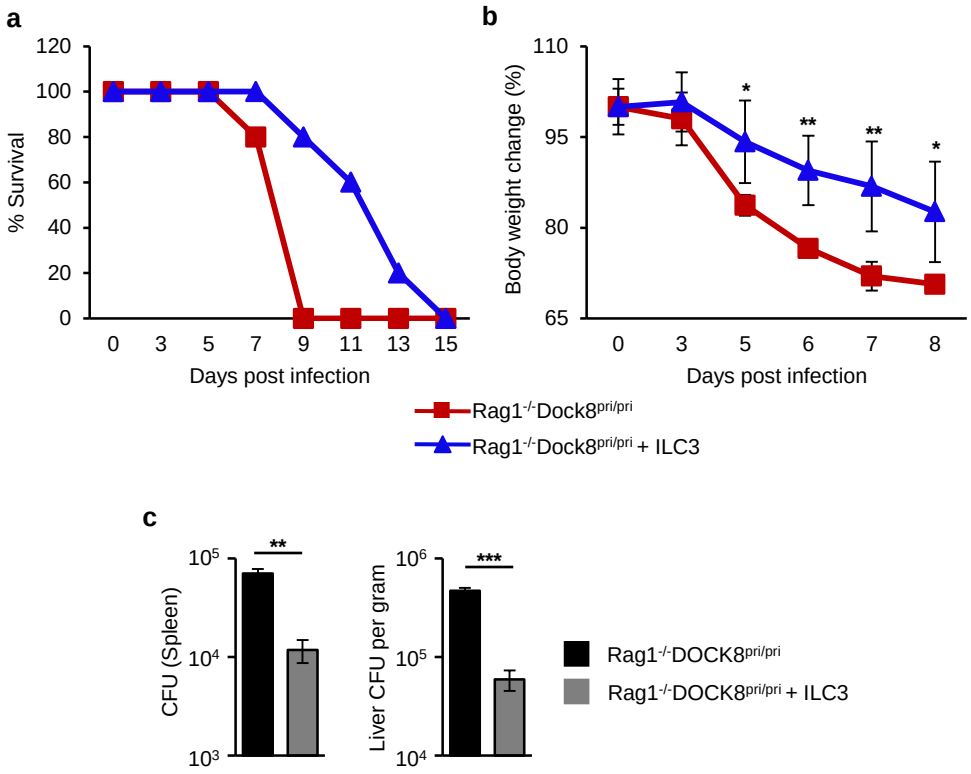

Supplementary Figure 12 ILC3s protect Rag1$^{-/-}$Dock8$^{pri/pri}$ mice from *C. rodentium* infection, related to figure 4. (a-c) CD90.2^{+}IL-23R^{+} (CD90.2^{+}GFP^{+}) ILC3s were sorted from the GI tract of Rag1$^{-/-}$IL-23R$^{gfp/+}$ mice and purified ILC3s were stimulated with IL-23 (25 ng/ml) and IL-1β (10 ng/ml) for 1 hour. Purified and In-vitro stimulated ILC3s were transferred by i.v. Injection (5 X 10^3 cells per mouse) into Rag1$^{-/-}$DOCK8$^{pri/pri}$ mice at day 0 after infection with 2 X 10^9 CFU of *C. rodentium*. Untreated Rag1$^{-/-}$DOCK8$^{pri/pri}$ mice were used as control. **(a)** Percent survival and **(b)** average body weight change after infection. **(c)** CFU in the spleens and livers of infected mice at day 7 post infection. Two independent experiments were performed with a minimum of five mice per group. The data shown are the mean ± SD. P-values were obtained by student's t-test. *p< 0.05, **p< 0.01, ***p< 0.001.

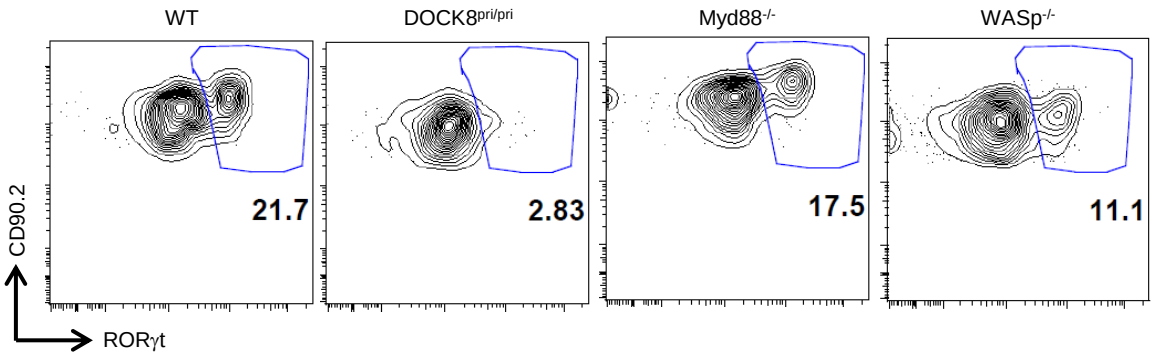

Supplementary Figure 13 Myd88 and WASp are dispensable RORγt$^+$ ILCs development, related to figure 4. RORγt$^+$ ILCs were analyzed in colonic LPLs from WT, DOCK8$^{pri/pri}$, Myd88$^{-/-}$ and WASp$^{-/-}$ by flow cytometry after gating on CD3$^-$CD90.2$^+$CD127$^+$ cells. Two independent experiments were performed with a minimum of three mice per group.

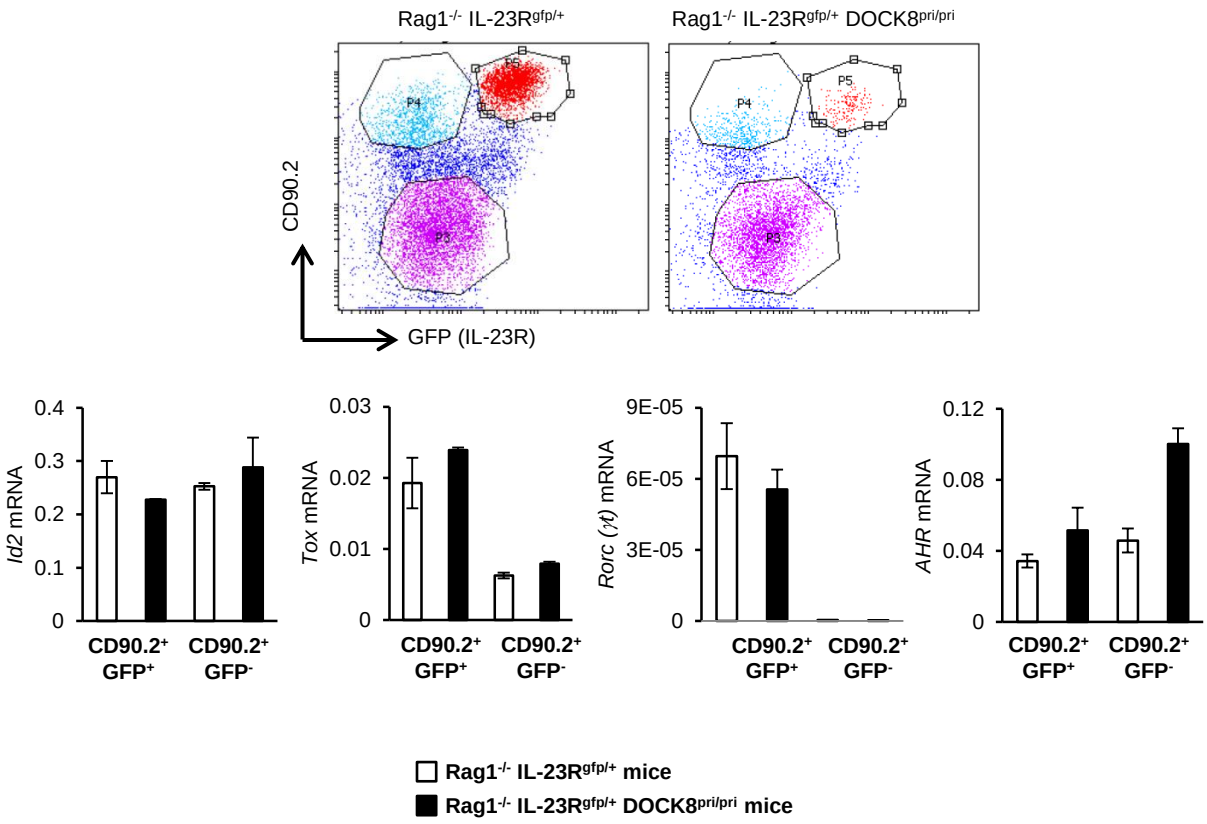

Supplementary Figure 14 Remaining DOCK8 deficient ILC3 have normal expression of *Id2*, *RORγt*, *AHR* and *Tox*, related to figure 5. CD90.2^{+}IL-23R^{-} (P4) and CD90.2^{+}IL-23R^{+} cells (P5) were purified from the SI LPLs of Rag1$^{-/-}$IL-23R$^{gfp/+}$ and Rag1$^{-/-}$IL-23R$^{gfp/+}$DOCK8$^{pri/pri}$ mice. Total RNA was extracted from purified cells with RNeasy mini kit (Qiagen) and reverse transcribed with the iScript cDNA synthesis kit (BioRad). The real time PCR was conducted using either SYBR Green (BioRad) reagents and primers as depicted in Table S1 or TaqMan Gene Expression Assay (Applied Biosystem): Ahr (Mm00478930) and Actb (Mm00607939). Gene expression was normalized as n-fold difference to the gene Actb. Two independent experiments were performed with pooled samples from four mice per group.

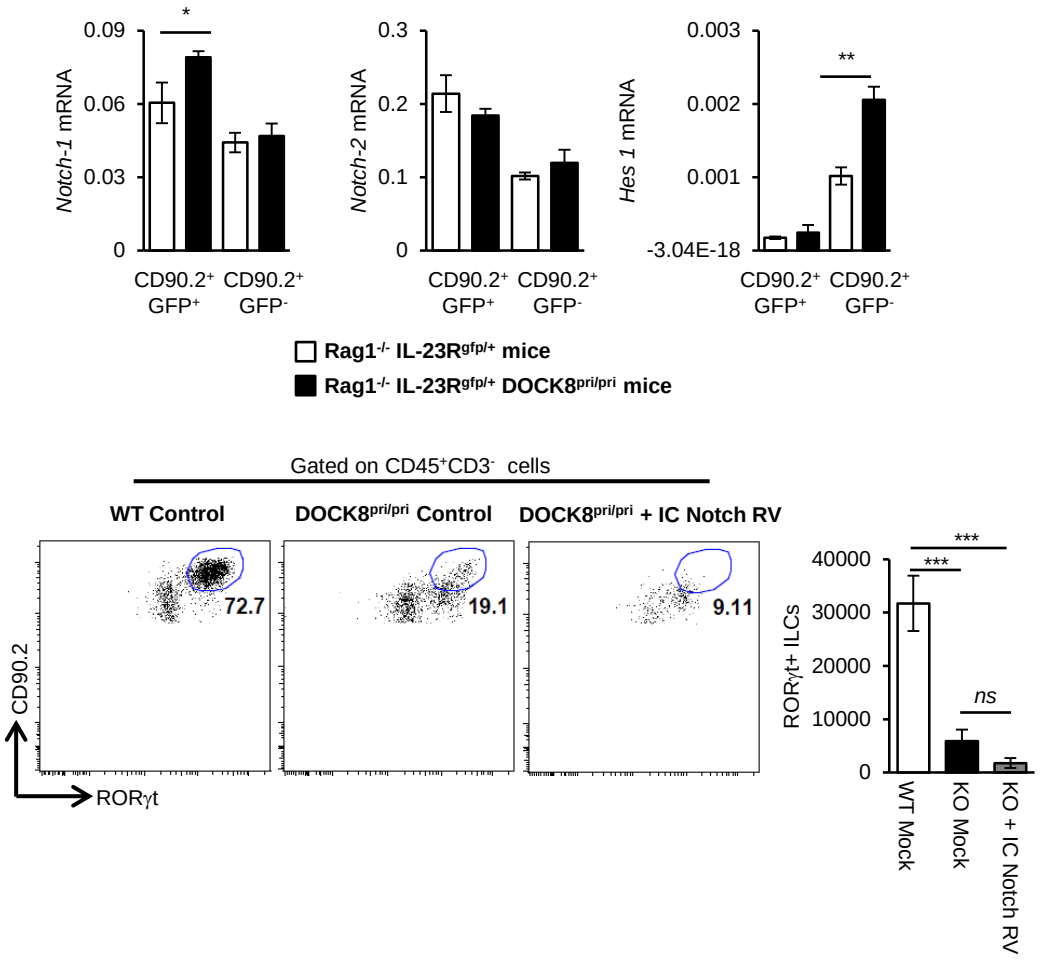

Supplementary Figure 15 Intracellular notch expression failed to rescue DOCK8 defect in RORγt$^+$ ILCs, related to figure 5. (Top panel) CD90.2$^+$IL-23R$^-$ and CD90.2$^+$IL-23R$^+$ (ILC3) cells were purified from the SI LPLs of Rag1$^{-/-}$IL-23R$^{gfp/+}$ and Rag1$^{-/-}$IL-23R$^{gfp/+}$DOCK8$^{pri/pri}$ mice. Total RNA was extracted from purified cells with RNeasy mini kit (Qiagen) and reverse transcribed with the iScript cDNA synthesis kit (BioRad). The real time PCR was conducted using primers and probe as depicted in Table S1. Gene expression was normalized as n-fold difference to the gene *RPL-19*. Two independent experiments were performed with a pooled samples from four mice per group. **(Bottom panel)** Dock8$^{pri/pri}$ mice bone marrow hematopoietic stem cells (HSCs) were transduced with intracellular domain of Notch (Notch IC) containing retrovirus (RV) and cotransplanted into lethally irradiated Rag2$^{-/-}$IL-2Rγ$^{-/-}$ recipients. Three weeks post HSCs transfer GI tract LPLs were analyzed for RORγt$^+$ ILCs. Frequency **(bottom left panel)** and absolute number **(bottom right panel)** of of RORγt$^+$ ILCs. Two independent experiments were performed with a minimum of three mice per group. The data shown are the mean ± SD. P-values were obtained by student's t-test. *p< 0.05, **p< 0.01 and ***p< 0.001. *ns*=not significant.

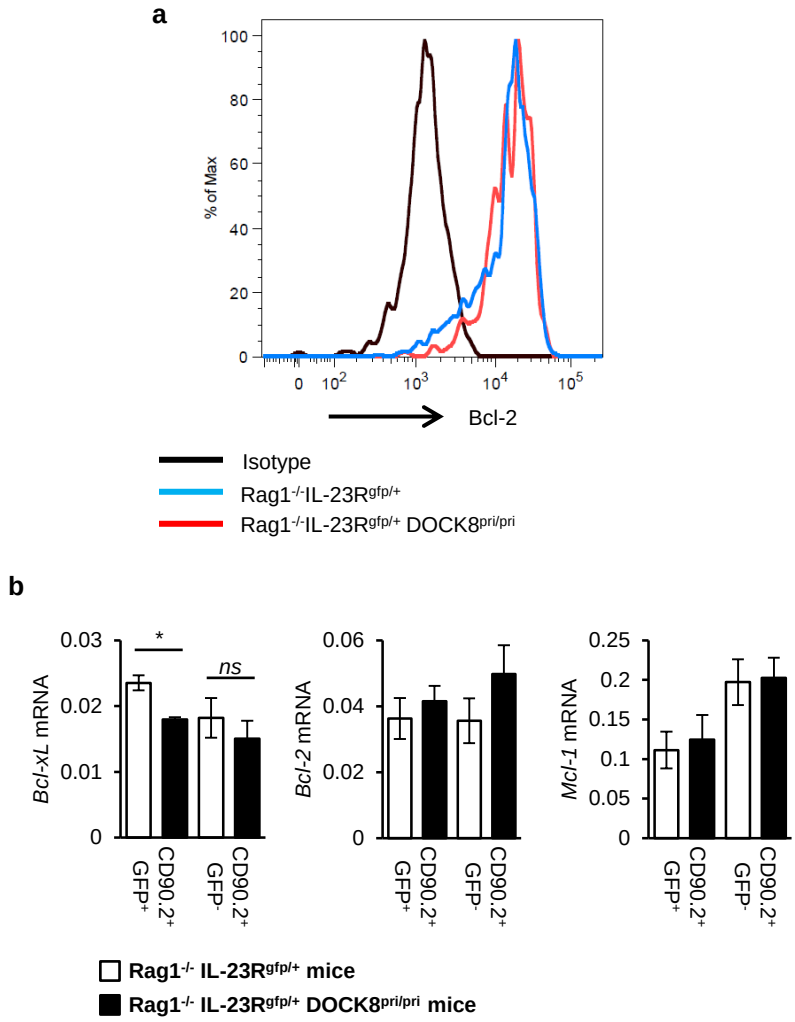

Supplementary Figure 16 Remaining DOCK8 deficient RORγt$^+$ ILCs have reduced expression of Bcl-xL , related to figure 5. (a) Bcl-2 expression on RORγt$^+$ ILCs were analyzed in GI tract LPLs from Rag1$^{-/-}$ and Rag1$^{-/-}$DOCK8$^{pri/pri}$ mice by flow cytometry after gating on CD90.2$^+$CD127$^+$RORγt$^+$ cells. **(b)** Quantitative PCR analysis of anti apoptotic genes Bcl-xL, Bcl-2 and Mcl-1 in CD90.2$^+$IL-23R$^-$ and CD90.2$^+$IL-23R$^+$ cells purified from the SI LPLs of Rag1$^{-/-}$IL-23R$^{gfp/+}$ and Rag1$^{-/-}$IL-23R$^{gfp/+}$DOCK8$^{pri/pri}$ mice. Total RNA was extracted from purified cells with RNeasy mini kit (Qiagen) and reverse transcribed with the iScript cDNA synthesis kit (BioRad). The real time PCR was conducted using SYBR Green (BioRad) reagents and primers as depicted in Supplementary table 1. Gene expression was normalized as n-fold difference to the gene RPL-19. Two independent experiments were performed with pooled samples from four mice per group. The data shown are the mean ± SD. P-values were obtained by student's t-test. *p< 0.05.

Singh et. al. **Supplementary Table 1. Primers for realtime PCR**

Primers	Sequence
mRPL-19	Forward, 5'-GCA TCC TCA TGG AGC ACA T-3'
	Reverse, 5'-CTG GTC AGC CAG GAG CTT-3'
	Probe, 5'-CTT GCG GGC CTT GTC TGC CTT-3' (FAM, TAMRA)
mIL-22	Forward, 5'-TCC GAG GAG TCA GTG CTA AA-3'
	Reverse, 5'-AGA ACG TCT TCC AGG GTG AA-3'
	Probe, 5'-TGA GCA CCT GCT TCA TCA GGT AGC A-3' (FAM, TAMRA)
RegIIIg	Forward, 5'-ATG GCT CCT ATT GCT ATG CC-3'
	Reverse, 5'-GAT GTC CTG AGG GCC TCT T-3'
	Probe, 5'-TGG CAG GCC ATA TCT GCA TCA TAC C-3' (FAM, TAMRA)
mIL-23p19	Forward, 5'-GGT GGC TCA GGG AAA TGT-3'
	Reverse, 5'-GAC AGA GCA GGC AGG TAC AG-3'
	Probe, 5'-CAG ATG CAC AGT ACT CCA GAC AGC AGC-3'(FAM, TAMRA)
IL-23R	Forward, 5'-ATGGTCTTGGGTACAGTATCG-3'
	Reverse 5'- CCATCTGGATGATATAGTGATA-3'
	Probe, 5'- CGTCCATCATTTCCAGGGTG-3' (FAM, TAMRA)
Id2	Forward, 5'-TCAGCCTGCATCACCAGAGA-3'
	Reverse 5'-CTGCAAGGACAGGATGCTGAT-3'
Tox	Forward, 5'-AGCCGAGCCAGGACTATGTG-3'
	Reverse 5'-GTGATGGGTGGGATGTTAAAATC-3'
Rorc	Forward, 5'-TCTACGCTATGAGGAAGGAAGGC-3'
	Reverse 5'-GACTATGGAGGAGAAACAGGTCCC-3'
mIL-17A	Forward, 5'-GCT CCA GAA GGC CCT CAG A-3'
	Reverse, 5'-CTT TCC CTC CGC ATT GAC A-3'
	Probe, 5'- ACC TCA ACC GTT CCA CGT CAC-3' (FAM, TAMRA)
Notch-1	Forward, 5'-ATGTCAATGTTCGAGGACCAG-3'
	Reverse, 5'-TCACTGTTGCCTGTCTCAAG-3'
Notch-2	Forward, 5'-GTGGCAGAGTTGATCAATTG-3'
	Reverse, 5'-ATATCTCTGTTGGCCCCATTC-3'
Hes1	Forward, 5'- GGCCTCTGAGCACAGAAAAAGT -3'
	Reverse 5'-GTGTTAACGCCCTCACACG -3'
Bcl-xL	Forward, 5'- TGGAGTAAACTGGGGTCGCATCG -3'
	Reverse 5'- AGCCACCGTCATGCCCGTCAGG -3'
Bcl-2	Forward, 5'- TGAGTACCTGAACCGGCATCT-3'
	Reverse 5'- GCATCCCAGCCTCCGTTAT-3'
Mcl-1	Forward, 5'- TCAAAGATGGCGTAACAAACTGG-3'
	Reverse 5'- CCCGTTTCGTCCTTACAAGAAC-3'